

Major Project Report

Synthesis and Characterization of Nanoparticles.



**UNIVERSITY OF PETROLEUM
& ENERGY STUDIES**

Submitted to

**Department of Mechanical Engineering
University of Petroleum and Energy Studies**

Mentor:-

**Dr. Rajnish Garg
Department of Mechanical Engineering**

By

Kunal Raj Sangal (R240211016)

Shashank Mudgal (R240211037)

Shubham Shroff (R240211024)

Varun Raturi (R240211027)

DECLARATION

We hereby declare that the work reported and submitted here in the Department of Mechanical Engineering is our work carried out under the supervision of Dr. Rajnish Garg. To the best of our knowledge and belief, no part of this work has been submitted here or elsewhere previously for the award of any other degree or diploma of this university or any other institute of higher learning. All sources of knowledge used and cited have been duly acknowledged.

Kunal Raj Sangal


Signature

Date: 04/05/15

Shashank Mudgal


Signature

Date: 04-05-15

Shubham Shroff


Signature

Date: 04/May/2015

Varun Raturi


Signature

Date: May 04, 2015

APPROVAL

This is to certify that the project entitled “**Synthesis and characterization of Nanoparticles**”, carried out by Kunal Raj, Shashank Mudgal, Shubham Shroff and Varun Raturi under my supervision has been read and approved for fulfilling the requirements and regulations governing the award of Bachelor of Technology Material Science with Specialization in Nano Technology of University of Petroleum and Energy Studies, Dehradun, India.

Supervisor Name: Dr. Rajnish Garg


Rajnish Garg
04/05/2015

Signature

DATE May 04, 2015

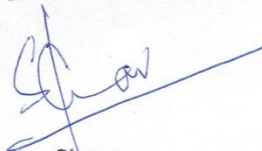
Coordinator Name: Dr. Subrahmanyam
Venkata Garimella


S. Venkata Garimella
04/05/15

Signature

DATE May 04, 2015

HOD Name: Dr. Suresh Kumar


S. Kumar

Signature

DATE May 04, 2015

Abstract

Al doped Strontium and Barium hexaferrite were prepared by Sol-Gel auto combustion method. $\text{SrFe}_{12-x}\text{Al}_x\text{O}_{19}$ and $\text{BaFe}_{12-x}\text{Al}_x\text{O}_{19}$ were prepared with $X=3$ and heat treated in a muffle furnace at 1000°C for 6 hours. The phase and crystal structure identification of the particles were done by using powdered X-ray diffraction which shows presence of hexaferrite phase and hexagonal crystal structure. The lattice parameter of the atomic structure decreases due to smaller aluminium ions replacing large iron ions. The size of the nanoparticles was measured by using Particle size analyzer. It shows that Al doped Strontium hexaferrite are smaller in size than barium hexaferrite. The dielectric properties were calculated by Vector Network Analyzer. The dielectric constant represents the absorbing power of the material. Strontium hexaferrite shows higher dielectric constant than barium hexaferrite hence has more absorbing capacity than barium hexaferrite. Overall, Al doped Strontium hexaferrite is more capable as radar absorbing material than Al doped barium hexaferrite.



List of symbols and abbreviations

θ	= Diffraction Angle
$^{\circ}\text{C}$	= Degree Celsius
Ba	= Barium
Sr	= Strontium
Al	= Aluminium
O	= Oxygen
RAM	= Radar Absorbing Material
XRD	= X-Ray Diffraction
M-type	= Magnetoplumbite
GHz	= Giga Hertz



List of figures

	Page No.
Figure 3.1 Sol Preparation	6
Figure 3.2 Gel preparation on magnetic stirrer	6
Figure 3.3 Ignition of the fire from the gel	7
Figure 3.4 Mortar and Pestle	7
Figure 3.5 Muffle furnace	8
Figure 3.6 Particle size analyzer	9
Figure 3.7 Bruker D8 Diffractometer	10
Figure 4.1 Synthesized Nanoparticles	11
Figure 4.2 XRD curve of Al doped barium hexaferrite	13
Figure 4.3 XRD curve of Al doped barium hexaferrite H.T. at 1000°C	14
Figure 4.4 XRD curve of Al doped Strontium hexaferrite	15
Figure 4.5 XRD curve of Al doped Strontium hexaferrite H.T. at 1000°C	16
Figure 4.6 Dielectric constant VS frequency curve of barium hexaferrite	17
Figure 4.7 Dielectric constant VS frequency curve of strontium hexaferrite	18

List of Tables

	Page No.
Table 3.1 Amount of chemical required for preparing Al doped Strontium hexaferrite	5
Table 3.2 Amount of chemical required for preparing Al doped barium hexaferrite	5
Table 4.1 Size of particles measured with particle size analyzer	11
Table 4.2 Calculations of peak from XRD curve of Al doped barium hexaferrite	13
Table 4.3 Calculations of peak from XRD curve of Al doped barium hexaferrite H.T at 1000 °C	14
Table 4.4 Calculations of peak from XRD curve of Al doped Strontium hexaferrite	15
Table 4.5 Calculations of peak from XRD curve of Al doped Strontium hexaferrite H.T. at 1000 °C	16
Table 4.6 Calculated Lattice parameters	17

Contents

	Page No.
ABSTRACT	iv
LIST OF SYMBOLS AND ABBREVIATIONS	v
LIST OF FIGURES	vi
LIST OF TABLES	vii
CHAPTER:1 INTRODUCTION	1
CHAPTER:2 LITERATURE REVIEW	2
2.1 OBJECTIVES	4
CHAPTER: 3 EXPERIMENTAL TECHNIQUES AND CHARACTERIZATION	5
3.1 MATERIALS USED	5
3.2 REACTION	5
3.3 SYNTHESIS	5
3.4 PARTICLE SIZE ANALYSIS	9
3.5 X-RAY DIFFRACTION SPECTROSCOPY	10
CHAPTER: 4 RESULTS AND DISCUSSION	11
4.1 SYNTHESIZED NANOPARTICLES	11
4.1 PARTICLE SIZE MEASUREMENT	11
4.2 XRD ANALYSIS	12
4.3 DIELECTRIC CONSTANT MEASUREMENT	17
CHAPTER:5 CONCLUSIONS AND FUTURE WORK	19
REFERENCES	20

CHAPTER: 1

Introduction

A lot of research work is being carried out on the synthesis of magnetic materials and making them useful for various applications. Many changes in the properties are attained in these magnetic materials at nano level. There are many methods to prepare magnetic nanoparticles such as Co-precipitation, Sol-Gel method, ball mill, Sonolysis and Hydro-thermal.

Ferrites have a technological interest as a permanent magnet and in magnetic recording media. The magnetic properties of ferrites are largely dependent on the microstructure and its processing routes. Various processes have been used to prepare ferrites, in which wet chemical method has advantages such as excellent product homogeneity, better compositional control and lower processing temperatures. Among these different chemical routes, the sol-gel auto combustion method has received considerable attention because of its relatively simple synthesis scheme. The M-type ferrites having magnetoplumbite structure are called hexagonal ferrites. These types of particle have high chemical stability and can be used as electromagnetic wave absorbers.

These materials have attracted much attention in past few years as they are used in Radar Absorbing Material (RAM). RAMs are of great interest because of their extensive applications in electronic devices such as computer, cell phones, local area network and laptops. Doping is done to enhance the properties of RAM. RAM has applications in the stealth technology of air craft, microwave dark rooms, military shielding, and missiles [1-4]. In previous decade, there have been many attempts to produce nano-RAMs, which have advantages over Micro-RAMs. Nano-RAMs have excellent absorption at broad bandwidths. Ability to spread as thin coating together with low density makes RAMs applicable for stealth aircrafts.

CHAPTER:2

Literature Review

There are various methods for synthesis of Aluminium doped Strontium Hexa-ferrite ($\text{SrFe}_9\text{Al}_3\text{O}_{19}$) and Barium Hexa-ferrite ($\text{BaFe}_9\text{Al}_3\text{O}_{19}$) nanoparticles. According to the data gathered from various research papers published, M-type ferrites are synthesized and characterized using following methods and techniques:

Electrochemical synthesis of magnetic nanoparticles using an undivided cell with two Fe electrodes, Energy dispersive X-ray microanalysis is done which confirms that they were composed of pure oxides. The size of the particles were under 50 nm observed by Transmission electron microscope. After heating for 1 hour at 300°C magnetic properties of hard ferrite are obtained [5].

Strontium ferrite ultra fine particles had been prepared using the micro emulsion processing. The mixed hydroxide precursor was obtained via co-precipitation of Sr^{2+} and Fe^{3+} in a water-in-oil micro emulsion of water. Phase analysis done by XRD shows that precursor yields pure hexaferrite after heat treating at 700 °C for 5 hours. From Transmission electron microscope, diameter of the particle was obtained as 50-100nm [6].

Sol-gel auto-combustion method has been used to synthesize ultra-fine particles of Strontium hexaferrite. The gels were prepared from metal nitrates and citric acid by various molar ratios of Fe/Sr and trimethylamine as pH adjusting agent. The size of the particles obtained from transmission electron microscope was 37nm [7].

Strontium hexaferrite ($\text{SrFe}_{12}\text{O}_{19}$) have been prepared by the sol-gel process. The prepared precursor was calcined with two different calcination techniques; using conventional furnace and microwave furnace. The average particle diagonal size of Strontium hexaferrite powder was 80-100 nm in conventional and 40-70 nm in microwave calcinations [8].

The fine particles of Strontium hexaferrite are synthesized by the hydrolysis of refluxed ethanol solution of Fe^{3+} and Sr^{2+} acetyl acetonates. The precipitates were then annealed to obtain a single magnetoplumbite phase. The average particle size of the annealed sample at 1173K was found to be in the range of 50-60nm [9].

The chemical co-precipitation and conventional ceramic method is used to synthesize the ultrafine particles of Strontium hexaferrite [10].

Synthesis of ultrafine particles of $\text{SrFe}_{12}\text{O}_{19}$ is done by citrate precursor technique. Solid state reactivity studies of citrate precursor led to the formation of fine particles of $\text{SrFe}_{12}\text{O}_{19}$ below 823 K. The size morphology of these particles was studied by Scanning electron microscope. The surface area measured for 5.2 nm crystallite was found to be $27.45\text{m}^2\text{g}^{-1}$. The average particle size was found to be 42 nm [11].

Highly Al^{3+} ion doped nano-crystalline $\text{SrFe}_{12-x}\text{Al}_x\text{O}_{19}$, were prepared by the auto combustion method and heat treated in air at 1100°C for 12h. The phase identification of the powders performed using x-ray diffraction show presence of high-purity hexaferrite phase and absence of any secondary phases. With Al^{3+} doping, the lattice parameters decrease due to smaller Al^{3+} ion replacing Fe^{3+} ions. Morphological analysis performed using transmission electron microscope show growth of needle shaped ferrites with high aspect ratio at Al^{3+} ion content exceeding $X > 2$ [12].

Sol-gel auto-combustion method has been adopted in the present work for synthesizing Strontium hexaferrite nanoparticles and Barium hexaferrite nanoparticles with aluminium doping because of an easy production technique and many advantages over other synthesizing methods like thin bond coatings to provide excellent adhesion between the metallic substrate and the top coat, thick coating to provide corrosion protection, production of high purity products because of the organo-metallic precursor of the desired ceramic oxides. It is a simple, economic and effective method for above applications.

2.1 Objectives

- Synthesis of Aluminium doped Strontium Hexa-ferrite ($\text{SrFe}_9\text{Al}_3\text{O}_{19}$) and Aluminium doped Barium Hexa-ferrite ($\text{BaFe}_9\text{Al}_3\text{O}_{19}$) nano particles by sol-gel auto combustion method.
- Heat treatment at 1000°C for 6 hours to remove volatile compounds and other impurities. Heat treatment gives pure M-type phase.
- Characterization by particle size analyzer and XRD.
- Comparison of the synthesized nano-particles on the basis of their dielectric properties.



CHAPTER: 3

Experimental Techniques and Characterization

The Aluminium doped Strontium and barium hexaferrite were prepared by Sol-Gel auto combustion method. Nitrate salts of each element are used for this process.

3.1 Materials used

Aluminium nitrate, Ferric nitrate, Strontium nitrate, Barium nitrate, Ammonia, Citric acid, distilled water.

3.2 Reactions

1. $\text{Sr}(\text{NO}_3)_2 + (12-X) \text{Fe}(\text{NO}_3)_3 + X \text{Al}(\text{NO}_3)_3 + \text{C}_6\text{H}_8\text{O}_7 + \text{NH}_3 = \text{SrAl}_x\text{Fe}_{12}\text{O}_{19} + \text{NH}_3\text{NO}_3 + \text{CO}_2 + \text{H}_2\text{O}$
2. $\text{Ba}(\text{NO}_3)_2 + (12-X) \text{Fe}(\text{NO}_3)_3 + X \text{Al}(\text{NO}_3)_3 + \text{C}_6\text{H}_8\text{O}_7 + \text{NH}_3 = \text{BaAl}_x\text{Fe}_{12}\text{O}_{19} + \text{NH}_3\text{NO}_3 + \text{CO}_2 + \text{H}_2\text{O}$

Based on above reactions, the amount required to produce desired amount of nanoparticles is given in Table- 3.1 and Table- 3.2

Table 3.1: Amount of chemical required for preparing Al doped Strontium hexaferrite.

Al content (x)	$\text{Sr}(\text{NO}_3)_2$	$\text{Fe}(\text{NO}_3)_3$	$\text{Al}(\text{NO}_3)_3$	$\text{C}_6\text{H}_8\text{O}_7$
3	2.11 gm	36.36 gm	11.253 gm	25 gm

Table 3.2: Amount of chemical required for preparing Al doped barium hexaferrite.

Al content (x)	$\text{Ba}(\text{NO}_3)_2$	$\text{Fe}(\text{NO}_3)_3$	$\text{Al}(\text{NO}_3)_3$	$\text{C}_6\text{H}_8\text{O}_7$
3	2.61 gm	36.36 gm	11.253 gm	25 gm

3.3 Synthesis

Step I- Sol preparation

As shown in Fig. 3.1, the solution of Aluminium doped Strontium hexaferrite is prepared by using ferric nitrate, aluminium nitrate and Strontium nitrate in calculated amounts. These

nitrate powder are kept in different beakers and further diluted using distilled water. All the nitrate solution is mixed in single beaker. Citric acid is added as a fuel for the auto combustion process. By adding citric acid the solution become acidic in nature so, its Ph is controlled by using ammonia. Same procedure is done for Barium.



Figure 3.1: Sol preparation

Step II- Gel preparation

Gel is prepared by putting the solution on magnetic stirrer with hot plate at 100°C for near about 3 hours as shown in Fig.3.2. After some time viscous gel is formed and rest of the water content is vaporized. Due to continuous stir the mixture also becomes homogeneous.

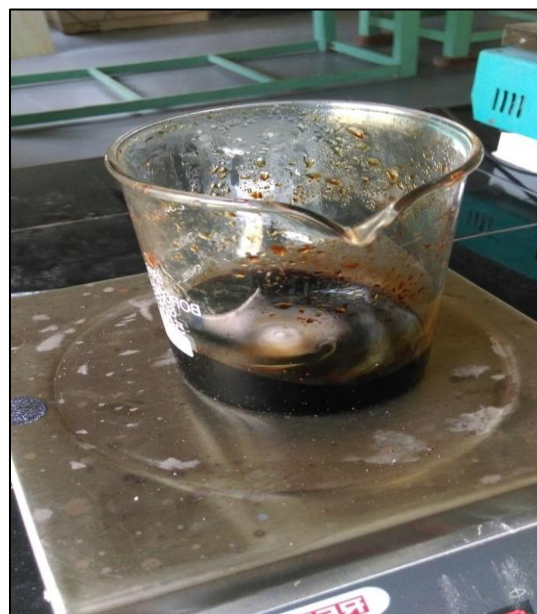
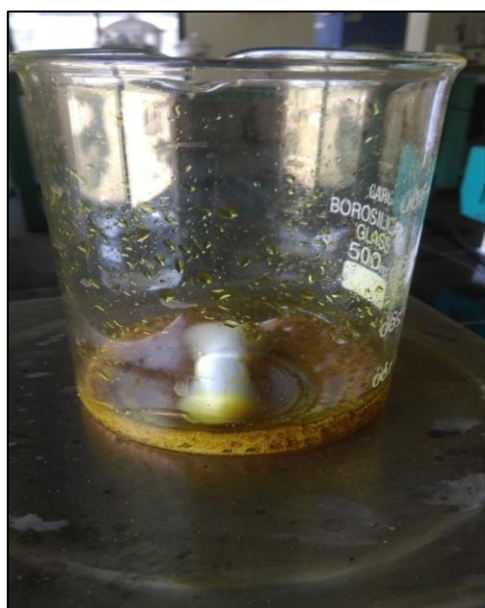


Figure 3.2: Gel preparation on magnetic stirrer

Step III- Auto combustion

Auto combustion is a self ignition process in which all the moisture in the gel is vaporised and xero-gel or ash is formed. When auto-combustion takes place, the gel in beaker catches fire and exhaustion takes place as shown in Fig 3.3. Due to this all the moisture in the gel vanishes.



Figure 3.3: Ignition of fire from the gel

Step IV- Preparing nano-particles from ash

After removal of moisture, xerogel is formed. This xerogel is a bulky structure containing ash or nanoparticles. Mortar and pestle shown in Fig.3.4 is used to convert the xerogel in fine form. The ash is crushed in mortar and pestle to convert it into powder form. It is a process like hand grinding.



Figure 3.4: Mortar and pestle

Step V- Heat treatment

Heat treatment is done to remove volatile compounds and other impurities. The muffle furnace used for heat treatment of nano particles is shown in Fig. 3.5.

The nanoparticles are placed in silica crucible. Silica crucible can bear high temperature without affecting the samples. Heat treatment converts amorphous phase to crystalline phase to give pure M-type ferrites which helps in better evaluation of properties of the ferrites by removing the unwanted compound.



Figure 3.5: Muffle furnace

3.4 Particle Size Analysis

The instrument model used for analysing the size of the nanoparticles was Zetasizer APS S90 which is shown in Fig.3.6. The Zetasizer Auto Plate Sampler automates particle size measurements from samples prepared in 96- or 384-well plates.

More specifically, the Zetasizer APS instrument provides the ability to measure size characteristics of particles or molecules in a liquid medium. This allows characterization of the particle size distribution to determine the presence and proportion of aggregates as a function of solvent and buffer conditions under optimum environmental conditions.

By using unique technology, particle size can be measured over a wide range of concentrations. The Zetasizer APS also has the ability to perform Trend measurements. The Zetasizer APS features pre-aligned optics and the precise temperature control necessary for reproducible, repeatable and accurate measurements.



Figure 3.6: Particle size analyzer

3.5 X-Ray Diffraction Spectroscopy

XRD is an indispensable method for materials investigation, characterization and quality control. The instrument model - Bruker D8 X-ray diffractometer, used for analyzing the crystal structure and lattice parameters is shown in Fig.3.7. The Bruker D8 X-ray diffractometer is designed to easily accommodate all X-ray diffraction applications in material research, powder diffraction and high resolution diffraction.



THE NATION BUILDERS UNIVERSITY

Figure 3.7: Bruker D8 Diffractometer

CHAPTER: 4

Results and Discussions

4.1 Synthesized Nanoparticles

The Aluminium doped Strontium Hexa-ferrite ($\text{SrFe}_9\text{Al}_3\text{O}_{19}$) and Barium Hexa-ferrite ($\text{BaFe}_9\text{Al}_3\text{O}_{19}$) nanoparticles synthesized by Sol-Gel auto-combustion method are shown in Fig 4.1. The weight measured after synthesis of nanoparticles was 12.3 grams for Barium Hexa-ferrite ($\text{BaFe}_9\text{Al}_3\text{O}_{19}$) and 11.4 grams for Strontium Hexa-ferrite ($\text{SrFe}_9\text{Al}_3\text{O}_{19}$).



Figure 4.1: Synthesized Nanoparticles

4.2 Particle size measurement

The particle size of synthesized nano powder as measured with Zetasizer is given in Table 4.1. It is clear from the results that the Strontium hexaferrite nanoparticles are smaller in size than Barium hexaferrite nanoparticles.

Table 4.1: Size of particles measured with particle size analyzer.

S.No.	SAMPLE	Size in nm
1	Al doped Barium Hexaferrite	498
2	Al doped Barium Hexaferrite Calcined at 1000°C	292
3	Al doped Strontium Hexaferrite	376
4	Al doped Strontium Hexaferrite Calcined at 1000°C	206

This is due to the fact that the atomic radius of Strontium is smaller than Barium. This is governed by the number of layers of electrons around the nucleus and the pull that the outer electrons feel from the nucleus.

In both cases, the two outer electrons feel a net pull of 2+ from the nucleus of both the elements. The negativity of the inner electrons cuts down the positive charge on the nucleus. This is true for all the Group 2 elements and therefore, the only factor which affects the size of the atom is the number of layers of inner electrons which have to be fitted in around the atom. It is obvious that more the layers of electrons are present, the more space they will take because electrons repel each other. This means that as one goes down the group, the atoms are bound to get bigger.

4.3 XRD Analysis

The variation in lattice parameter of both the nanoparticles, before and after their heat treatment as measured by the Bruker D8 diffractometer is given in Table 4.6. It is clear from the results that Barium Hexaferrite nanoparticles showed a very minute decrease in lattice parameter at 1000°C and a similar kind of increment was observed in case of Strontium Hexaferrite nanoparticles at the same temperature.

This distortion in lattice parameter is governed by the small atomic size of Aluminium as the lattice distortion is not invariant but size dependent.

The XRD graphs for both Barium and Strontium hexaferrites, before and after their heat treatment are shown in figures: 4.2 - 4.5 respectively. The peaks generated in these graphs corresponds to the standard peaks generated in case of Ferrites. The calculations from these respective graphs are given in Tables: 4.2 - 4.5. The lattice parameters given in Table 4.6 were calculated from these graphs and tables. The results from XRD spectroscopy clearly indicates that both Barium and Strontium hexaferrites nanoparticles belong to m-type Ferrites.

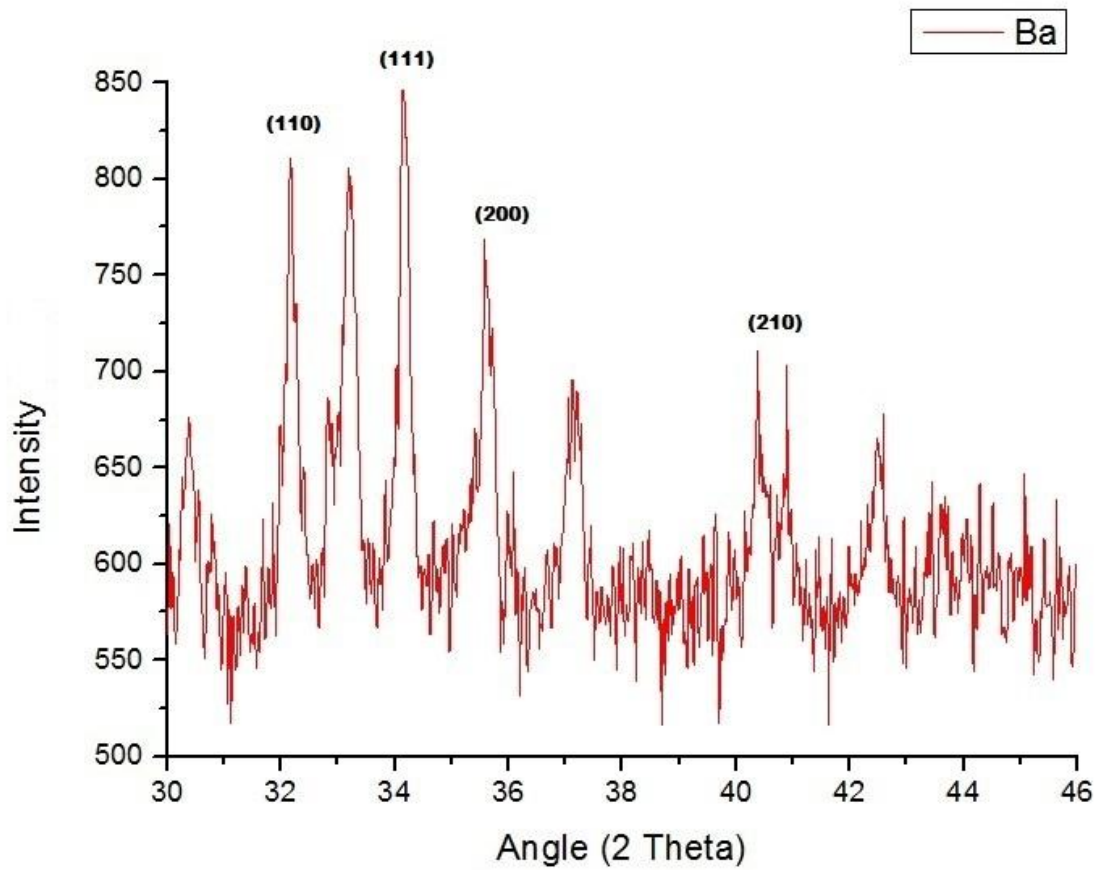


Figure 4.2: XRD graph of Al doped barium hexaferrite

THE NATION BUILDERS UNIVERSITY

Table 4.2: Calculations of peak from XRD curve of Al doped barium hexaferrite

2 Θ	Θ (deg)	$\sin \Theta$	$\sin^2 \Theta$	Ratio	K factor	$h^2+k^2+l^2$	hkl
32.1788	16.0894	0.2771	0.07678441	1	2.378964213	2	110
33.1955	16.59775	0.2856	0.08156736	1.062290639	3.186871918	3	111
34.1557	17.07785	0.2936	0.08620096	1.122636223	3.367908668	3	111
35.7184	17.8592	0.3066	0.09400356	1.224253205	3.672759614	4	200
37.1493	18.57465	0.3185	0.10144225	1.321130813	3.963392439	4	200
40.3876	20.1938	0.3451	0.11909401	1.551018104	4.653054311	5	210

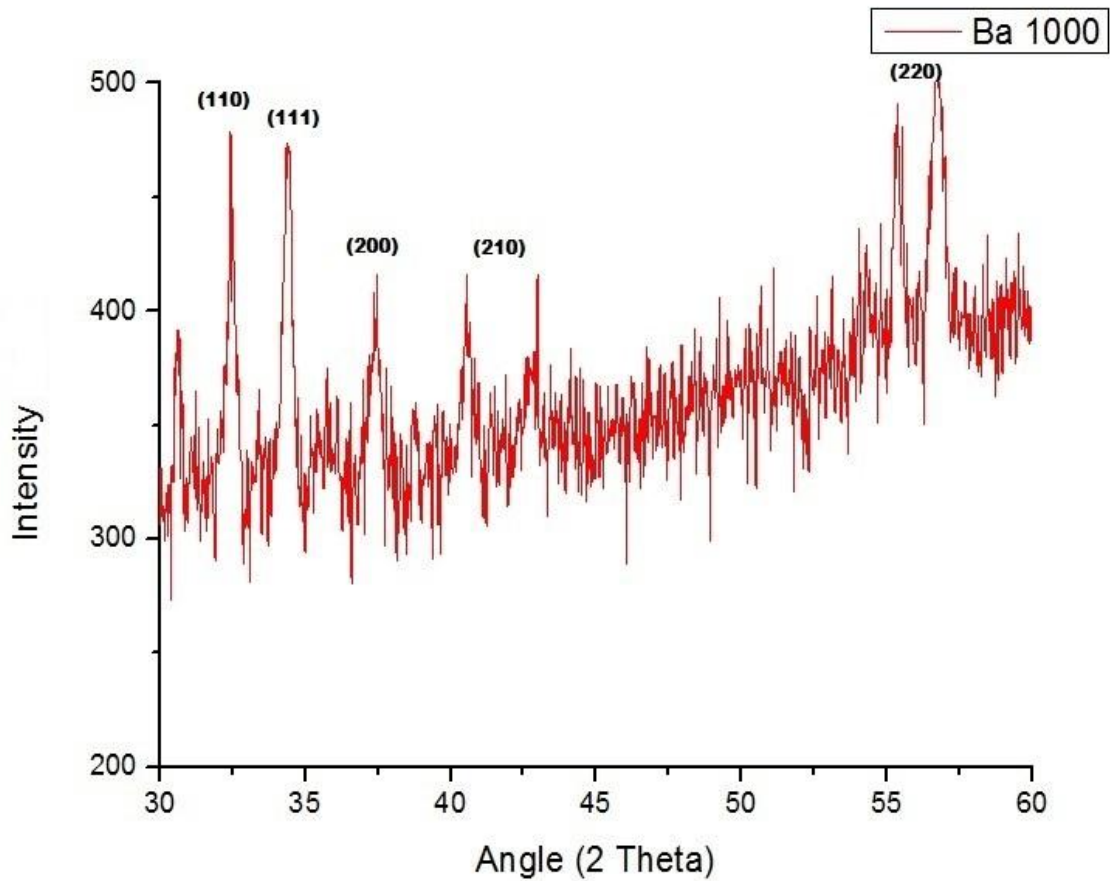


Figure 4.3: XRD graph of Al doped barium hexaferrite H.T. at 1000°C

THE NATION BUILDERS UNIVERSITY

Table 4.3: Calculations of peak from XRD curve of Al doped barium hexaferrite H.T. at 1000 °C

2 Θ	Θ (deg)	$\sin \Theta$	$\sin^2 \Theta$	Ratio	k factor	$h^2+k^2+l^2$	hkl
32.4612	16.2306	0.2795	0.07812025	1	2.35949844	2	110
34.4193	17.20965	0.2958	0.08749764	1.12003789	3.360113671	3	111
37.3752	18.6876	0.3204	0.10265616	1.314078744	3.942236232	4	200
40.557	20.2785	0.3465	0.12006225	1.536890243	4.610670729	5	210
42.6092	21.3046	0.3633	0.13198689	1.689534916	5.068604747	5	210
55.2801	27.64005	0.4639	0.21520321	2.754768578	8.264305734	8	220

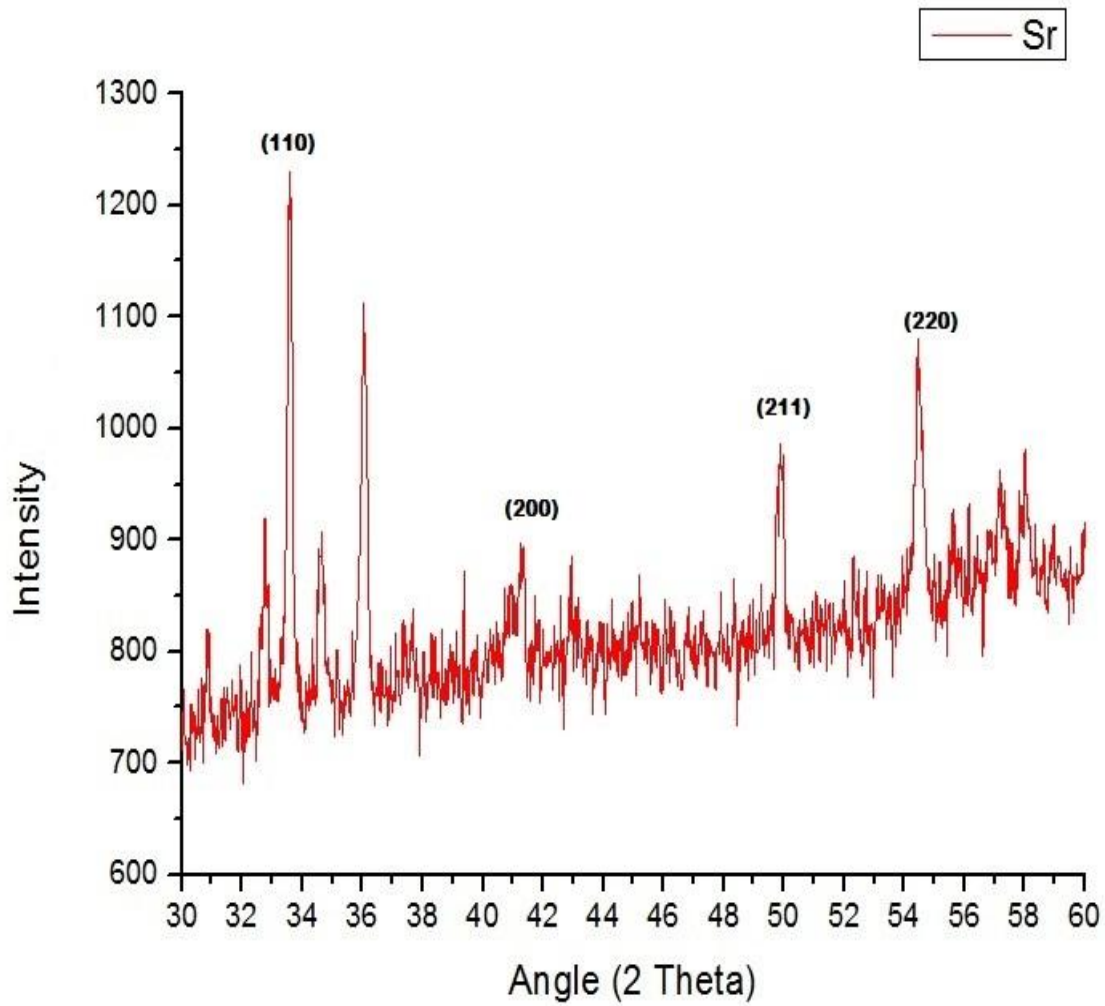


Figure 4.4: XRD graph of Al doped Strontium hexaferrite

Table 4.4: Calculations of peak from XRD curve of Al doped Strontium hexaferrite

2 Θ	Θ (deg)	$\sin \Theta$	$\sin^2 \Theta$	Ratio	k factor	$h^2+k^2+l^2$	hkl
33.6097	16.80485	0.28911	0.083584592	1	2.323849446	2	110
36.0384	18.0192	0.30933	0.095685049	1.144768988	3.434306964	3	111
41.2537	20.62685	0.3522	0.12404484	1.484063473	4.452190418	4	200
49.952	24.976	0.4222	0.17825284	2.132604054	6.397812163	6	211
54.4517	27.22585	0.4574	0.20921476	2.503030221	7.509090662	8	220

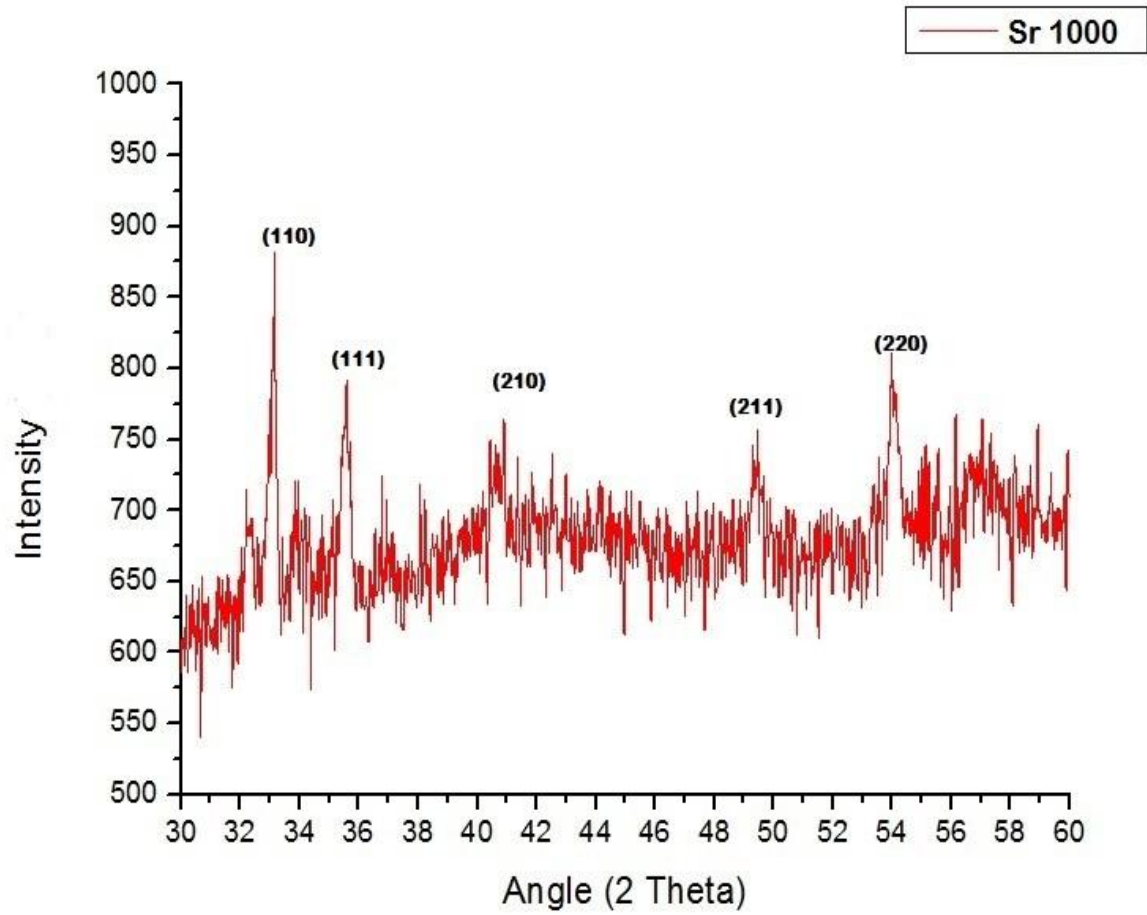


Figure 4.5: XRD graph of Al doped Strontium hexaferrite H.T. at 1000°C

Table 4.5: Calculations of peak from XRD curve of Al doped Strontium hexaferrite H.T. at 1000 °C

2 Θ	Θ (deg)	$\sin \Theta$	$\sin^2 \Theta$	Ratio	k factor	$h^2+k^2+l^2$	hkl
33.1578	16.5789	0.2853	0.08139609	1	2.31555144	2	110
35.5866	17.7933	0.3055	0.09333025	1.146618345	3.439855035	3	111
40.9148	20.4574	0.3495	0.12215025	1.500689407	4.50206822	5	210
49.4813	24.74065	0.4185	0.17514225	2.15172805	6.45518415	6	211
54.1505	27.07525	0.4551	0.20711601	2.544544953	7.633634859	8	220

Table 4.6: Calculated Lattice parameters

SAMPLE	Lattice Parameter ; a in Å	Lattice Parameter ; c in Å
Ba	4.80	7.48
Ba Heat treated	4.76	7.33
Sr	4.40	6.82
Sr Heat treated	4.96	7.60

4.4 Dielectric constant measurement

The variations in dielectric constants of both the nanoparticles, before and after their heat treatment are shown in Fig. 4.6 and Fig. 4.7 respectively. The results suits for the application of Strontium Hexaferrite and Barium Hexaferrite nanoparticles as RAMs. In case of Strontium hexaferrite, maximum dielectric constant value of 7.46 was achieved at all frequencies in X-band range but for Barium hexaferrite maximum dielectric constant value of 6.72 was achieved at a single frequency of 8.53 GHz in the X band range. Both the materials got their maximum value when annealed at 1000°C for 6 hrs.

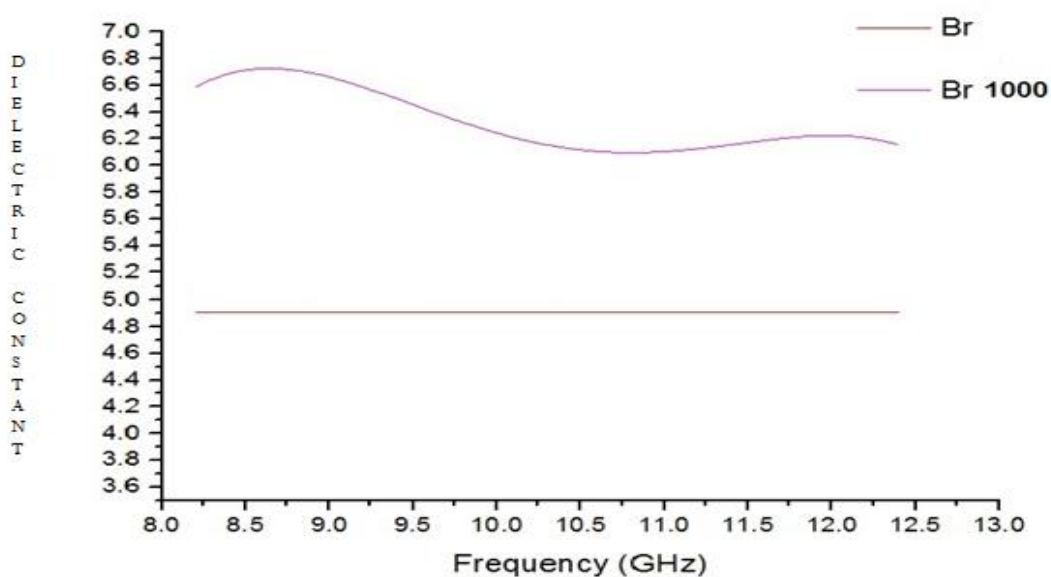


Figure 4.6: Dielectric constant VS frequency curve of barium hexaferrite

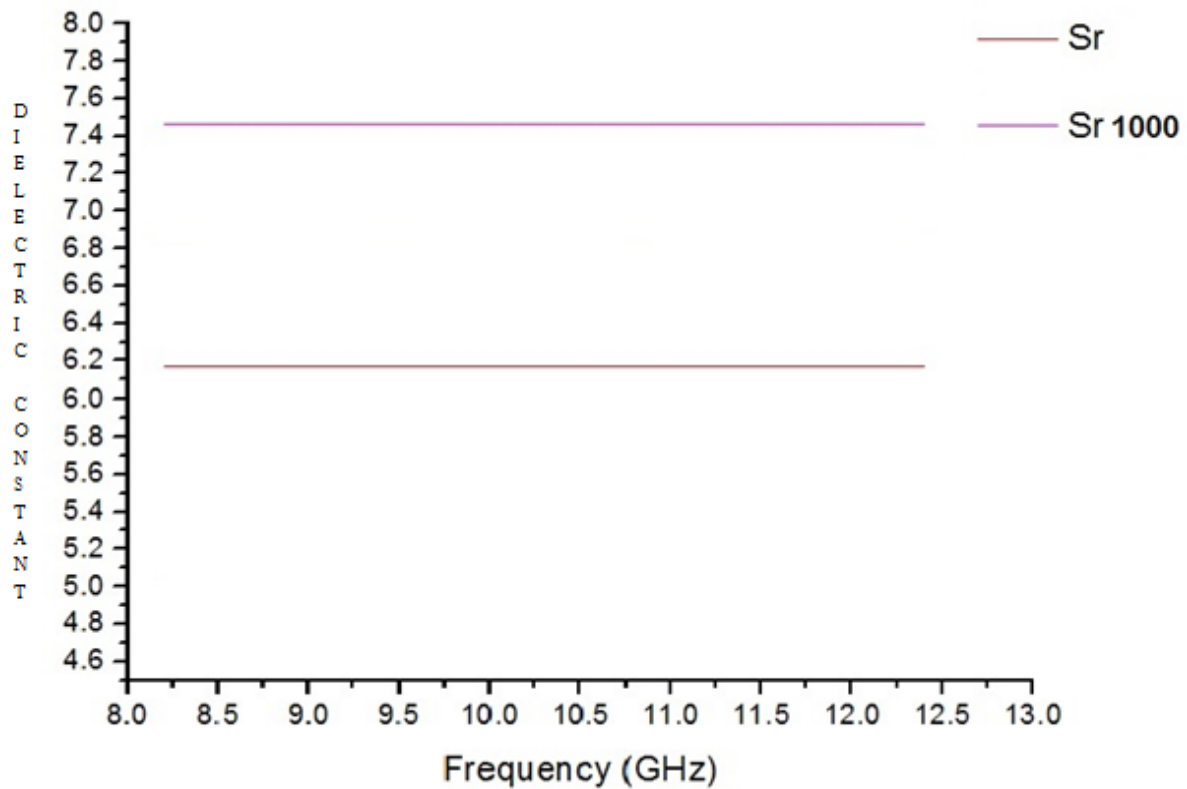


Figure 4.7: Dielectric constant VS frequency curve of Strontium hexaferrite

The measurement of complex dielectric properties of materials at radio frequency has gained increasing importance. The effect of such a systematic morphological transformation of nanoparticles on dielectric properties (complex permittivity and permeability) and microwave absorption properties are estimated in X band (8.2–12.2GHz). When compared, it was observed that the dielectric constant of Strontium hexaferrite nanoparticles was more than that of Barium hexaferrite nanoparticles, which in turn, resulted in the fact that Barium hexaferrite nanoparticles are better radar wave absorbing particles than Strontium hexaferrite nanoparticles.

The values of dielectric constants for both the nanoparticles is governed by the fact that as the temperature increases or the annealing is done for these type of materials, their dielectric property improve because of particle size effect i.e. when the nanoparticles are heated its size increases and they agglomerate with each other due to which polarization increases. When electric charges do not flow through the material, it slightly shifts from its equilibrium position and polarization occurs. This is the reason for different values of dielectric constants of both the nanoparticles.

CHAPTER: 5

Conclusion and Scope for Future work

It can be concluded from the work that:

- Strontium hexaferrite nanoparticles are smaller in size than Barium hexaferrite nanoparticles. This is due to the fact that the atomic radius of Strontium is smaller than Barium.
- Barium Hexaferrite nanoparticles showed a very minute decrease in lattice parameter whereas a small increment was observed in case of Strontium Hexaferrite nanoparticles at the same temperature. The distortion in lattice parameter is governed by the small atomic size of Aluminium as the lattice distortion is not invariant but size dependent.
- The dielectric constant of Strontium hexaferrite nanoparticles was more than dielectric constant of Barium hexaferrite nanoparticles. This is because as the temperature increases or the annealing is done for these types of materials, their dielectric property improves because of particle size effect.
- Barium hexaferrite nanoparticles are better radar wave absorbing particles than Strontium hexaferrite nanoparticles as it depends on the dielectric constant values for both the materials.

As far as the future aspects of ferrites are concerned, very few materials with such wide ranging properties exist and therefore, ferrites are unique magnetic materials which find applications in almost all fields, for example, the Polycrystalline Ferrites holds the reputation of being an irreplaceable magnetic material because of their precious contribution in technological applications. Ferrites are such a class of important electromagnetic-wave absorbing materials, of which magnetoplumbite and spinel hexagonal ferrites are the most widely used materials.

Ferrites exhibit dielectric properties i.e. they let electromagnetic waves to pass through them, and so do not readily conduct electricity. Hence in many applications, Ferrites are usually preferred over electrically conducting materials like Iron, Nickel and other transition metals.

In future, the doping of rare earth metals such as Lanthanum, Neodymium, Yttrium etc. can be used for biomedical applications such as bio-imaging.

References

1. J.R. Liu, M.Itoh, T.Horikawa, M.Itakura, N.Kuwano, K.I.Machida, *Journal of Physics D Applied Physics*, 37 (19) (2004)2737–2741.
2. X.F.Zhang, X.L.Dong, H.Huang, Y.Y.Liu, W.N.Wang, X.G.Zhu, *Applied Physics Letters* 89(5) (2006)053115-1053115-3.
3. X.F.Zhang, X.L.Dong, H.Huang, Y.Y.Liu, B.Lv, J.P.Lei, *Journal of Physics D applied Physics*, 40(17)(2007)5383–5387.
4. L.J. Deng, M.G. Han, *Applied Physics Letters* 91 (2007) 023119.
5. C.G. Koops, “On the Dispersion of resistivity and Dielectric Constant of Some Semiconductors at Audio frequencies”, *Phys. Rev.* 83(1), pp. 121-124, 1951.
6. K.W. Wagner, “The Distribution of Relaxation Times in Typical Dielectrics”, *Ann. Physics* 40, pp. 817-819, 1973.
7. P. Chen, R-X. Wu, J. Xu, A. Jiang and X. ji, “Effect of Magnetic Anisotropy on the Stop Band of Ferromagnetic Electromagnetic Band Gap Materials”, *Journal of Physics: Condensed matter*, 19, 106205(7pp), 2007.
8. X. Liu, W. Zhong, S. Yang, Z.Yu, B. Gu, Y. Du, “ Influence of La³⁺ Substitution on the Structure And Magnetic Properties of M-Type Strontium Ferrites”, *Journal of Magnetism and Magnetic Materials*, 238, pp. 207-214, 2002.
9. I. Perelshtein, N. Perkas, Sh. Magdassi, T. Zioni, M. Royz Z. Maor, A. Gedanken, “ Ultrasound- Assisted Dispersion of SrFe₁₂O₁₉ Nanoparticles in Organic Solvents and the use of the Dispersion as Magnetic Cosmetic”, *J. Nanopart Res*, 10, pp. 191-195, 2008.
10. F.M.M. Pereira, M.P. Santos, R. S.T.M. Sohn, J.S. Almeida, A.M.L. Medeiros, M.M. Costa, A.S.B. Sombra, “ Magnetic and Dielectric Properties of the M-type ferrites Chapter 5 Page 151.
11. C.M. Fang, F. Kools, R. Meteselaar, G.de. With and R.A de Groot, “Magnetic and Electronic Properties of Strontium Hexaferrite Srfe12o19 from First Principles Calculations”, *Journal of Physics: Condensed Matter*, 15, pp. 6229-6237, 2003.
12. H.Luo, B.K.Rai, et.al. “Physical and magnetic properties of highly aluminium doped Strontium ferrite nanoparticles prepared by auto-combustion route”, *Journal of magnetism and magnetic materials*, 324 (2012) 2602–2608.